Asymmetric Shock Wave Generation in a Microwave Rocket Using a Magnetic Field

Masayuki Takahashi

Department of Aeronautics and Astronautics, The University of Tokyo, Bunkyo-ku 113-8656, Japan

E-mail: m.takahashi@al.t.u-tokyo.ac.jp

Abstract. A plasma pattern is reproduced by coupling simulations between a particle-in-cell with Monte Carlo collisions model and a finite-difference time-domain simulation for an electromagnetic wave propagation when an external magnetic field is applied to the breakdown volume inside a microwave-rocket nozzle. The propagation speed and energy-absorption rate of the plasma are estimated based on the breakdown simulation, and these are utilized to reproduce shock wave propagation, which provides impulsive thrust for the microwave rocket. The shock wave propagation is numerically reproduced by solving the compressible Euler equation with an energy source of the microwave heating. The shock wave is asymmetrically generated inside the nozzle when the electron cyclotron resonance region has a lateral offset, which generates lateral and angular impulses for postural control of the vehicle. It is possible to develop an integrated device to maintain beaming flight of the microwave rocket, achieving both axial thrust improvement and postural control, by controlling the spatial distribution of the external magnetic field.

1. Introduction

It is necessary to develop innovative launch schemes to promote utilization of small satellites because the launch timings and orbits of small satellites are restricted in conventional launch schemes when sharing a chemical rocket with a main satellite. A microwave propulsion system has been proposed to realize frequent and flexible launches of small satellites while reducing the launch cost through repetitive launches of inexpensive vehicles [1–5]. Intense microwaves are radiated from a ground-based oscillator to a thruster equipped with a parabolic mirror, and the incident beam is focused by the mirror to induce air breakdown by the strong fields in the focal region. A dense plasma is generated by the gas breakdown and propagates toward the nozzle exit while forming strong shock waves because the energy absorbed by the plasma is transferred to neutral particles through the collision process. The vehicle obtains an impulsive thrust from interactions between the thruster wall and the shock waves. Chemical fuel aboard the vehicle can be removed or reduced because ambient air acts as the fuel, which decreases the launch cost.

Pressure dependencies of the breakdown structure and the thrust performance of a microwave rocket were assessed previously by placing a parabolic thruster in a vacuum chamber [2, 3, 6]. A discrete plasma was formed at atmospheric pressure because a standing wave was induced in front of the plasma due to waves reflected by the overcritical plasma. On the other hand, the breakdown pattern became diffusive at lower pressures because rapid electron diffusion smeared out the plasma pattern. The propagation speed of the ionization front was found to increase with

decreasing ambient pressure due to the rapid diffusion of electrons. The thrust performance of the microwave rocket degraded at lower pressures because the propagation speed of the ionization front became faster and the energy-absorption rate of the plasma decreased. It is necessary to suppress the propagation speed of the ionization front and improve the energy-absorption rate in order to enhance the generated shock wave inside the rocket nozzle at lower pressures. The breakdown pattern of the microwave plasma was numerically reproduced by coupling fluid or particle models of plasma transport with electromagnetic wave propagation [7–9]. Based on a fully kinetic simulation, it was proposed to apply an external magnetic field to the breakdown volume in order to confine the plasma inside the rocket nozzle [9]. Axial thrust performance was improved at lower pressures because electron cyclotron resonance (ECR) heating was combined with plasma confinement [10, 11].

In addition to improving axial thrust, it is necessary to obtain postural control impulses in order to maintain beam-riding flight [12–14]. The generated thrust is drastically degraded if the incident beam has lateral and angular misalignments with respect to the vehicle axis. The vehicle finally deviates from the incident beam axis if restoring forces for diminishing incidental misalignments are not attained during flight. The capturing ability of the incident beam, which is called beam-riding performance, is crucial to maintaining higher thrust and stable flight without deviation from the beam line. The beam-riding performance is evaluated entirely by the vehicle's feedback abilities against lateral and angular offsets from the incident beam line. The "lightcraft" vehicle, which has an annular shroud in order to generate the centering-feedback force, was proposed by Myrabo [12], and flight demonstrations of the lightcraft were conducted using high-averaged-power repetitive-pulses. The lightcraft was passively pushed back toward the center of the incident beam because the blast wave interacted with the ring-shaped shroud when the incident beam encountered lateral misalignment. However, the lightcraft, weighting 50 g, deviated from the incident beam line because of insufficient angular feedback performance, and its flight altitude was only 71-m altitude in 2001. It is necessary to propose an active control scheme for beam riding because passive control such as that of the lightcraft cannot maintain stable flight in a repetitive-pulse launch.

The objective of this study is propose an active control technique for maintaining stable flight of a beamed-energy propulsion vehicle. To actively control the lateral and angular impulses acting on the vehicle, it is necessary to deform the generated shock wave by controlling the spatial distribution of energy absorption by the plasma. The asymmetric energy-absorption region can be obtained when the magnetic field is asymmetrically applied to the breakdown volume inside the rocket nozzle. The lateral and angular impulses are evaluated using CFD code when the asymmetric shock wave interacts with the thruster.

2. Numerical Methods

A one-dimensional (1D) particle-in-cell with Monte Carlo collisions (PIC-MCC) model is coupled with a finite-difference time-domain (FDTD) simulation to reproduce the breakdown structure induced by microwave irradiation when the external magnetic field is applied to the discharge volume. The propagation speed and energy-absorption rate of the plasma are evaluated in the discharge simulation. The axial, lateral, and angular impulses are assessed using computational fluid dynamics (CFD) code by reproducing shock wave generation and reflection by the thruster wall.

2.1. Electromagnetic wave propagation

Electromagnetic wave propagation and interaction with the plasma are reproduced using the 1D FDTD method to examine the breakdown pattern, propagation speed of the ionization front, and energy-absorption rate of the plasma. Maxwell's equations are numerically solved to simulate electromagnetic wave propagation. For the boundary conditions of the FDTD simulation, a Mur

absorption boundary [15] is utilized to model the open boundary by damping the electromagnetic waves. A total field-scattered field implementation is employed to inject microwaves into the computational domain. The current density **J** in the Ampere-Maxwell law is evaluated in the 1D PIC-MCC simulation to introduce interactions between the motion of the charged particles and the microwave oscillations.

2.2. Fully kinetic simulation with collision reactions

The external magnetic field is applied to the breakdown volume to enhance electron heating by satisfying the ECR condition. The PIC method is utilized to reproduce interactions between the cyclotron motions of the charged particles and microwave oscillations during microwave breakdown. The 1D simulation is performed with three velocity (3V) components to reduce the computational load for simulating the collisional plasma. In the 1D3V PIC module, the equations of motion for the electron and ion particles are temporally integrated using the Buneman-Boris method [16] to predict the charged-particle motions. The current density $\mathbf{J} = qn\mathbf{v}$ is assessed on computational grids using linear weighting of super-particles in the PIC module and is fed back into Maxwell's equations in the FDTD simulation. The microwave reflection and damping caused by the plasma are reproduced by the feedback of the current density to Maxwell's equations. Collision reactions between the electron and neutral particles are introduced by combining the MCC model with the PIC method. The Nanbu method [17] is used to evaluate the existence or non-existence and the reaction types of the collisions. Eighteen reactions (e.g., elastic collision, vibrational excitation, rotational excitation, electron-impact excitation, and ionization) are introduced in the MCC model based on Phelps's cross section for nitrogen gas [18]. The MCC model is coupled with the PIC model using the Birdsall method [19].

2.3. Shock wave propagation induced by gas heating

A shock wave is induced inside a microwave-rocket nozzle when the microwave energy absorbed by the plasma is transferred to the energy of the neutral particles. The energy absorbed by the plasma is evaluated by the PIC-MCC and FDTD coupling simulation and deposited into a source term in the fluid simulation to reproduce the propagation of shock waves. The two-dimensional (2D) Euler equations are numerically integrated to reproduce the shock wave propagation around the microwave rocket as follows:

$$\frac{\partial \mathbf{Q}}{\partial t} + \frac{\partial \mathbf{E}}{\partial x} + \frac{\partial \mathbf{F}}{\partial y} = \mathbf{S}, \tag{1}$$

where **Q** is a conservative vector, **E** and **F** are inviscid flux vectors in the x- and y-directions, and **S** is the heating term estimated by the PIC-MCC calculation. Discretization is performed in a cell-centered finite-volume manner [20]. The AUSM-DV method [21] is employed for numerical fluxes with the second-order MUSCL method [22]. In the MUSCL method, characteristic variables are selected as interpolation quantities and a minmod limiter is used to fulfill the TVD condition. Time integration for unsteady shock wave propagation is performed using the first-order explicit Euler method.

3. Simulation Conditions

3.1. FDTD and PIC-MCC coupling simulation

The maximum intensity of the incident field E_y is fixed at 5 MV/m, and the microwave frequency is 110 GHz following Hidaka's experiments [6]. The 1D simulation domain has 2.25λ (the microwave wavelength is $\lambda = 0.27$ cm), and the number of grid points used is 40,000 in order to resolve the Debye length of the electrons. The initial plasma spot, which has a Gaussian distribution, is set on the computational domain to simplify the first gas breakdown under microwave focusing. The microwaves are injected from the left boundary ($x = 0$ cm) to reproduce microwave-plasma interaction. An external magnetic field B_z is applied to the computational

domain to confine electron transport while the incident electric field E_y oscillates in the y-direction. ECR heating occurs when the external magnetic field is chosen as 3.93 T because oscillation of the electric field E_y is coupled with the electron cyclotron motion twinning around the magnetic field B_z. The ambient pressure is set as 0.003 atm to obtain a large Hall parameter.

3.2. CFD simulation to reproduce shock wave propagation

A cylinder-type microwave rocket is numerically modeled to estimate the lateral and angular impulses obtained by microwave irradiation using CFD code. The nozzle radius is 3 cm and its length L is 18 cm following Oda's experiments [2,3]. The distance between the center of gravity and the nozzle head is 7.2 cm. The absorption energy and propagation speed of the ionization front are calculated by the PIC-MCC and FDTD coupling simulation in order to introduce the energy source into the CFD simulation. An external magnetic field has a lateral offset (Fig. 1); however, the incident beam has no offset in this simulation. The magnetic field satisfying the ECR condition is applied into only 253 cm $\leq y \leq$ 256 cm (the nozzle axis exists at $y = 253$ cm). However, there is no magnetic field at 250 cm $\leq y <$ 253 cm to generate the asymmetric shock wave. The heating region moves from the nozzle head toward the nozzle exit ($x = 193$ cm) at the propagation speed of the ionization front. Microwave irradiation is terminated when the heating region at the ECR condition reaches the nozzle exit. The slip boundary condition is used on the thruster wall, and the other outer boundaries are treated as zeroth-order extrapolations. The axial, lateral, and angular impulses are calculated by integrating the surface pressures on the thruster walls. The lateral force is defined in the positive y-direction, and the clockwise direction is taken to be positive for the angular impulse.

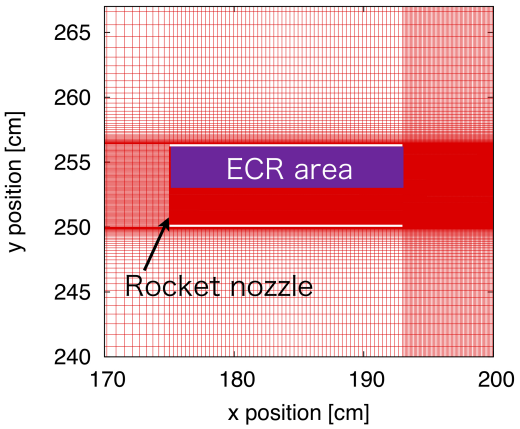

Figure 1. Computational grid of rocket nozzle. ECR magnetic field is applied with a lateral offset against the nozzle axis.

4. Results

4.1. Propagation speed and energy-absorption rate of plasma

5-MV/m, 110-GHz microwaves are irradiated onto an initial plasma spot at an ambient pressure of 0.003 atm. An external magnetic field of 3.93 T is applied to the discharge volume to induce ECR heating by satisfying $\omega = \omega_c$, where ω is the incident microwave frequency and ω_c is the electron cyclotron frequency. The breakdown structure, propagation speed of the ionization front, and energy-absorption rate of the plasma are assessed using the PIC-MCC and FDTD coupling simulation to model an energy source in the CFD simulation.

At 0 T, the electron density is small at an ambient pressure of 0.003 atm because of infrequent ionization collisions. The incident microwaves penetrate into the plasma spot because the electron density does not exceed the cut-off density for microwave reflection (Fig. 2(a)). However, the incident microwaves are reflected by overcritical plasma when a magnetic field of 3.93 T is applied to the discharge volume because electron-impact ionization rapidly occurs due to high-energy electrons generated by ECR heating (Fig. 2(b)). The ionization front propagates toward the microwave source by repeated microwave reflection, electron diffusion, and ionization at the plasma front. By tracing the position of the ionization front, the propagation speeds are evaluated as 1,430 km/s and 1,250 km/s at magnetic fields of 0 T and 3.93 T, respectively, at an ambient pressure of 0.003 atm. The energy-absorption rate of the plasma is estimated by tracing the electron energy at the plasma front in order to model the source term in the shock wave simulation. At 0 T and 3.93 T, the energy-absorption rates by the plasma are assessed as 3.3×10^{11} W/m^3 and 5.0×10^{13} W/m^3, respectively. The shock wave induced by the microwave irradiation is reproduced based on the propagation speed and the energy-absorption rate evaluated by the PIC-MCC and FDTD coupling simulation.

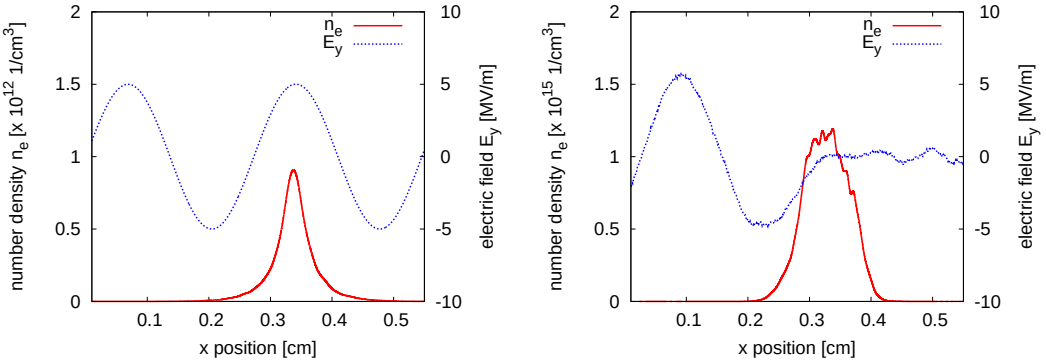

(a) 0 T, 1.6 ns (b) 3.93 T, 1.6 ns

Figure 2. Electron number density and electric field at 0.003 atm. 5-MV/m, 110-GHz microwaves are irradiated onto the initial plasma spot, and microwave plasma propagates toward the microwave source (left boundary). Electrons and ions diffuse in the x-direction, and the incident microwave field oscillates in the y-direction. External magnetic fields B_z of 0 T and 3.93 T are applied in the z-direction.

4.2. Lateral and angular impulses driven by asymmetric shock waves

A shock wave is induced inside the microwave-rocket nozzle when microwaves are irradiated onto the vehicle because the microwave energy absorbed by the plasma is transferred to the energy of neutral particles through collisional reactions. The shock wave is enhanced when a magnetic field satisfying the ECR condition is applied to the breakdown volume because the energy-absorption rate is improved by resonant heating. An asymmetric shock wave is induced when the applied magnetic field has a lateral offset relative to the vehicle axis (the ECR condition is satisfied at 253 cm $\leq y \leq$ 256 cm, while the vehicle axis exits at $y = 253$ cm), which provides lateral and angular impulses to the thruster for achieving postural control.

The shock wave is asymmetrically generated inside the rocket nozzle because the energy-absorption region caused by the ECR heating is asymmetric due to the lateral offset of the external magnetic field (Fig. 3(a)). Lateral and angular impulses are not obtained when the lateral offset of the magnetic field does not exist; however, the thruster obtains lateral and angular impulses with a lateral offset because the asymmetric shock wave interacts with the

rocket nozzle (Fig. 3(b)). Negative lift is generated because the asymmetric shock wave strongly interacts with the side wall at $y = 250$ cm. An anti-clockwise moment is obtained because the high pressure of the shock wave interacts with the nozzle corner at $(x,\ y) = (175\text{ cm},\ 250\text{ cm})$. The amplitude and direction of the lateral and angular impulses can be controlled if the offset of the magnetic field is changed by controlling the current density of an external coil. The axial thrust is also improved because the shock wave enhanced by ECR heating interacts with the nozzle head. It is possible to develop an integrated device that can achieve axial thrust improvement and postural control by applying an external magnetic field onto a microwave-rocket nozzle.

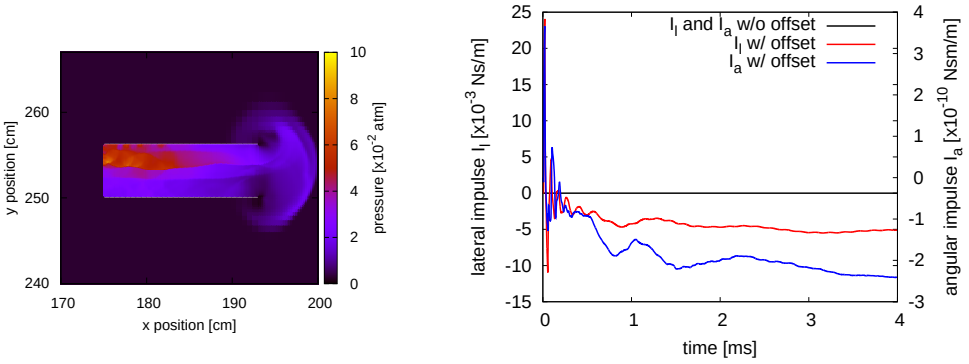

(a) pressure distribution (b) lateral and angular impulses

Figure 3. Pressure distribution around the microwave rocket and lateral and angular impulses. The axis of microwave irradiation is aligned with the vehicle axis. An external magnetic field is applied to the breakdown volume with and without a lateral offset.

5. Conclusion

By coupling the PIC-MCC model with FDTD simulation, the propagation speed and the energy-absorption rate of plasma were estimated for the case where an external magnetic field is applied into the discharge volume induced by microwave irradiation. The breakdown pattern was reproduced and shock wave propagation was reproduced using CFD code based on the propagation speed and the energy-absorption rate of the plasma. An asymmetric shock wave was induced inside the microwave-rocket nozzle when the ECR region had a lateral offset, providing lateral and angular impulses for postural control of the vehicle. In addition to axial thrust enhancement, postural control can be conducted by utilizing an external magnetic field satisfying the ECR condition.

Acknowledgments

The fully kinetic simulations in this work were performed on a Silicon Graphics International (SGI) Altix UV1000 at the Advanced Fluid Information Research Center, Institute of Fluid Science, Tohoku University. The fluid simulations in this work were performed on a FUJITSU PRIMEHPC FX100 at the Japan Aerospace Exploration Agency. This work was supported by JSPS KAKENHI Grant Number JP16J09910.

References

[1] Nakagawa T, Mihara Y and Komurasaki K 2004 *J. Spacecraft and Rockets* **41** (1) 151–153
[2] Oda Y and Komurasaki K 2006 *J. Appl. Phys.* **100** 113307
[3] Oda Y 2008 *Doctor Thesis* (Tokyo: The University of Tokyo)

[4] Fukunari M, Komatsu R, Arnault A, Yamaguchi T, Komurasaki K and Arakawa Y 2013 *Vacuum* **88** 155–159
[5] Fukunari M, Arnault A, Yamaguchi T and Komurasaki K 2014 *Appl. Optics* **53** (31) 16–22
[6] Hidaka Y, Choi E M, Mastovsky I, Shapiro M A, Sirigiri J R and Temkin R J 2009 *Phys. Plasmas* **16** 055702
[7] Boeuf J P, Chaudhury B and Zhu G Q 2010 *Phys. Rev. Lett.* **104** 015002
[8] Kourtzanidis K, Boeuf J P and Rogier F 2014 *Phys. Plasmas* **21** 123513
[9] Takahashi M and Ohnishi N 2014 *Appl. Phys. Lett.* **105** 223504
[10] Takahashi M and Ohnishi N *Trans. Japan Soc. Aero. Space Sci., Aero. Tech. Japan* (accepted)
[11] Takahashi M and Ohnishi N 2016 *J. Appl. Phys* **120** 063303
[12] Myrabo L N, Messitt D G and Mead F B Jr 1998 *AIAA Paper* 98-1001
[13] Kenoyer D A, Anderson K S and Myrabo L N 2008 *Beamed Energy Propulsion: Fifth International Symposium on Beamed Energy Propulsion, AIP Conference Proceedings* vol 997 (New York: American Inst. of Physics) pp 325–337
[14] Scharring S, Eckel H A and Röser H P 2011 *Int. J. Aero. Innovations* **3** (1) 15–31
[15] Mur G 1981 *IEEE Trans. EMC* **EMC-23** (4) 377–382
[16] Buneman O 1967 *J. Comput. Phys.* **1** 517–535
[17] Nanbu K 1994 *Jap. J. Appl. Phys.* **33** 4752–4753
[18] Phelps A V 2008 *Compilation of Electron Cross Sections* (University of Colorado) [http://jila.colorado.edu/∼avp/collision_data/electronneutral/ELECTRON.TXT]
[19] Birdsall C K 1991 *IEEE Trans. on Plasma Sci.* **27** 65–85
[20] Hirsch C 1984 *Numerical Computation of Internal and External Flows* vol 1 (New York: John Wiley and Sons) pp 237–266
[21] Wada Y and Liou M S 2006 *AIAA Paper* 2006-1358
[22] van Leer B 1979 *J. Comput. Phys.* **32** (1) 101–136